Using Electromagnetic Time Reversal Similarity Metric to Locate Lightning-Originated Flashovers on Overhead Transmission Lines

Zhaoyang Wang[†], Francesco Gerini[‡], Mario Paolone[§], Carlo Alberto Nucci[‡] and Farhad Rachidi[†]
[†]Electromagnetic compatibility (EMC) Laboratory, Swiss Federal Institute of Technology, Lausanne (EPFL), Switzerland
[‡]Department of Electrical, Electronic and Information Engineering, University of Bologna, Italy
[§]Distributed Energy System Laboratory (DESL), Swiss Federal Institute of Technology, Lausanne (EPFL), Switzerland

***Abstract*—The paper presents a method to locate flashovers resulting from direct lightning strikes to overhead transmission lines. The method exploits the electromagnetic time-reversal theory and uses the cross-correlation between the flashover-originated transient current observed in the direct time and the transverse branch currents in the reversed time at the guessed flashover locations as a similarity metric to identify the location of the flashover. The performance of the similarity metric is numerically illustrated using two simulation case studies associated with a shielding failure and a back-flashover.**

Index Terms*— *Direct lightning strikes; electromagnetic time reversal; flashovers; transmission lines.

I. Introduction

Power supply interruptions and equipment damages are largely correlated to various weather-related causes and, in particular, to direct lightning strikes on overhead power transmission lines [1]–[6].

As known, the lightning incidence to overhead transmission lines is estimated by means of its so-called lightning exposure, which concerns the physical processes involved in the final stage of the progression of the downward lightning leader. Such a progression can result in strikes to phase conductors, towers or overhead ground wires (OHGWs) [1], [2]. The injection of lightning return stroke currents into these conductors generates high voltage lightning surges, which propagate as traveling waves starting from the location of the lightning attachment point, towards both directions along the transmission line.

In an occurrence of a direct lightning strike near power substations, the lightning surge can cause damage to transformer windings and even to the devices at the secondary side [1], [2]. Apart from such rare occasions, direct lightning strikes may originate flashovers (in case of shielding failure) and back-flashovers [1]. In such events, the most obvious effects are voltage sags or permanent power outages. Yet, another fact that cannot be ignored is the insulation deterioration of the network components during the flashover occurrence. The weakness of insulation strength is effectively a hidden danger, which needs to be identified as early as possible and eliminated by routine maintenance [1], [2]. Thus, accurate location of lightning-originated flashover occurrences is of fundamental importance in power supply security.

Within this context, a number of methods have been developed to identifying the point of a lightning strike to overhead transmission lines as well as the location of flashovers (e.g., [7]–[9]), including a recent method based on the Electromagnetic Time Reversal (EMTR) theory [9]. EMTR has found other applications in power systems such as locating lightning discharges (e.g., [10], [11]) and various disturbances in power networks [12]–[15].

The EMTR method (e.g., [9]) takes advantage of the time-reversal invariance of the wave equations in transmission lines and the associated inherent time-reversal spatial correlation property [16]–[18]. More specifically, locating flashovers in power networks is realized by time-reversing the flashover-originated electromagnetic transients and back-injecting them into a numerical model of the system under study from original observation point(s). The time-reversed back-propagated transients converge at the flashover location. The converging behavior is quantified by the energy of the transverse branch current at guessed flashover locations [9].

Very recently, a novel EMTR metric, named the maximum of the cross-correlation sequence (MCCS), was proposed [19]. The MCCS metric exploits EMTR-based time-domain similarity characteristics. Its applicability to locate faults in power networks is discussed in [19] and has been shown to be more effective with respect to the metric calculating the energy of the fault current.

This paper aims to extend the application of the MCCS (or similarity) metric to locate flashovers resulting from a direct lightning strike to overhead transmission lines. The paper is structured as follows. Section II briefly summarizes the time-domain similarity of electromagnetic transients in the EMTR theory. Then, the algorithm to compute the similarity metric is proposed. Section III presents the modeling hypotheses considered in the simulations used to validate the proposed metric. In Section IV, the simulation results are presented and discussed. Section V concludes the paper with final remarks.

II. Similarity Characteristics in Electromagnetic Time Reversal Theory

A. Similarity characteristics

Within the context of locating faults in power networks, it has been demonstrated in [19] that the fault current [denoted as $I_{x_f}^{\mathrm{RT}}(t)$[1]] observed in the reversed time at the real fault location exclusively behaves as a quasi-scaled and time-delayed copy of the time-reversed back-injected transient current [denoted as $I_0^{\mathrm{TR}}(t)$]. Based on this observation, in [19] a cross-correlation metric has been proposed to quantitatively represent the level of similarity between $I_0^{\mathrm{TR}}(t)$ and $I_{x_\mathbb{G}}^{\mathrm{RT}}(t)$, $x_\mathbb{G}$ being *a priori* defined guessed fault locations (GFLs)[2].

$$x_\mathbb{G} = \left\{ x_g \middle| x_{g,1}, x_{g,2}, \ \ldots \ , x_f, \ \ldots \right\}. \tag{1}$$

The real fault location (i.e., $x = x_f$) is characterized by the maximum of the cross-correlation calculated at various GFLs.

In the next subsection, we illustrate a specific algorithm to adapt the EMTR method to the focus of this paper, namely locate direct lightning strike originated flashovers occurring along overhead transmission lines.

B. MCCS or similarity metric

The use of the EMTR-based similarity characteristic to locate flashovers resulting from direct lightning strikes can be summarized into a three-step algorithm. Note that, the algorithm uses a single observation point (OP).

i) As a result of a direct lightning strike to a transmission line, the originated transient voltage is measured at a given observation point (e.g., the primary substation that supplies the transmission line) starting from a triggering instant $t_{trigger}$:

$$V_0^{\mathrm{DT}}(t), \ t \in [t_{trigger}, \ t_{trigger} + T], \tag{2}$$

where T is the time window over which $V_0^{\mathrm{DT}}(t)$ is recorded.

The observation point is located at one of the network terminals, which is generally assumed to be the origin of space coordinate system [i.e., subscript '0' of the observed voltage in (2)].

ii) The high-frequency transient [denoted as $\tilde{V}_0^{\mathrm{DT}}(t)$] is extracted using appropriate filtering (i.e., to remove steady-state industrial frequency component) within a temporal window T_w^{DT}, and time reversed as

$$V_0^{\mathrm{TR}}(t) = \tilde{V}_0^{\mathrm{DT}}(-t + T_w^{\mathrm{DT}}), \ t \in [0, \ T_w^{\mathrm{DT}}]. \tag{3}$$

The transients are transformed into a Norton equivalent by

$$I_0^{\mathrm{TR}}(t) = V_0^{\mathrm{TR}}(t)/Z_0. \tag{4}$$

where Z_0 is the input impedance of the terminal (transformer), assumed to be a high resistance [9], [12].

iii) The current flowing through a transverse branch, which is located at each pre-defined location among $x_\mathbb{G}$, is numerically simulated by back-injecting the current $I_0^{\mathrm{TR}}(t)$ into a numerical model of the network from the observation point.

The proposed time-domain similarity metric consists of calculating the cross-correlation between $I_0^{\mathrm{TR}}(t)$ and $I_{x_\mathbb{G}}^{\mathrm{RT}}(t)$. For formulating the metric precisely, we take the following factors into consideration: *i)* power networks generally feature multiple conductors (phase conductors and possibly shielding wires), and *ii)* both acquired and simulated signals are discretely sampled. As a result, we define two signal sequences:

$$\phi(k) \triangleq I_{0,\,ph}^{\mathrm{TR}}(k \cdot \Delta t), \tag{5}$$

$$\psi(x_\mathbb{G}, \ k) \triangleq I_{x_\mathbb{G},\,ph}^{\mathrm{RT}}(k \cdot \Delta t), \tag{6}$$

with

$$k = 0, \ 1, \ 2, \ \ldots, \ K, \tag{7}$$

and

$$K = T_w^{\mathrm{DT}}/\Delta t. \tag{8}$$

where Δt is the time sampling interval. In (5) and (6), the additional subscript 'ph' numbers phase-conductors.

Given this, the MCCS metric can be calculated by

$$R_{\phi,\,\psi}^m(x_\mathbb{G}, \ l) = max\left[\sum_{k=0}^{K} \phi(k) \cdot \psi(x_\mathbb{G}, \ k - l)\right] \tag{9}$$

with

$$l = 0, \ \pm 1, \ \pm 2, \ \ldots, \ \pm (K - 1). \tag{10}$$

Among the *a priori* guessed flashover locations (GFLs) $x_\mathbb{G}$, the most likely position of x_f is determined by

$$x_f = arg\Big|_{x_\mathbb{G}} \quad max\left[R_{\phi,\,\psi}^m(x_\mathbb{G}, \ l)\right] \tag{11}$$

III. Modeling and Simulation Approach

The simulation study in this paper makes use of the EMTP-RV simulation environment. This section presents the approaches to: *i)* model the different elements composing typical overhead transmission lines, and *ii)* simulate the electromagnetic transient (EMT) process initiated by a lightning strike causing flashovers.

A. Transmission lines

The simulations presented in this paper consider typical 220-kV single-circuit overhead transmission lines. The adopted line parameters are summarized in TABLE I.

The frequency-dependent (FD) line model takes into account the frequency dependence of the line parameters and thus achieve sufficient accuracy of simulating the EMT processes originated by a flashover occurrence (in the direct time) as well as simulating the transverse branch current in the reversed time.

In the following simulations, the EMTP-RV built-in FD line module is used to model the transmission lines.

[1]The superscript RT is customarily used to represent the reversed time. Similarly, the stage wherein an event (e.g., faults or flashovers) occurs is named direct time in the time reversal theory, and is abbreviated as DT.

The subscript is used to indicate the spatial coordinate where the signal is observed.

[2]In the following texts, GFLs ($x_\mathbb{G}$) is also used to refer to guessed flashover locations. Similar use applies to x_f to denote the real flashover location.

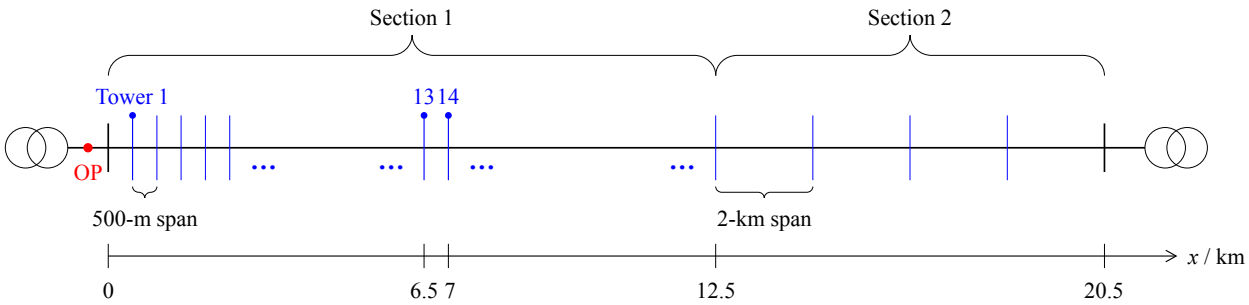

Fig. 1: Schematic representation of the transmission line considered in the simulation case studies. The overhead-line towers represented by the blue line segments are defined as guessed flashover locations. Two tower spacings are considered: 500 m in Section 1, and 2 km in Section 2.

TABLE I: Main Electrical Parameters of the Transmission Line

Parameter	Value	Unit
Diameter of the phase conductor	5.26	cm
Diameter of the OHGW	1.1	cm
DC resistance of the phase conductor	0.067	Ω/km
DC resistance of the OHGW	3.605	Ω/km
Soil conductivity	0.1	S/m

B. Transformers

According to the previous studies on the use of EMTR-based methods to locate various disturbances in power networks (e.g., [9], [12], [14]), power transformers can be represented by their high-frequency input impedances with magnitudes of some tens to hundreds of kΩ. In the presented simulations, the transformer is represented with a 10-kΩ resistance per phase.

C. Overhead-line tower

The overhead-line towers are simulated using a built-in tower model in the EMTP-RV environment. The model offers a simplified representation of typical single-circuit overhead-line towers by considering the tower as a vertical conductor modeled by distributed parameter lines [1], [20], [21]. The tower in the simulated 220-kV circuit is a 30.7-m long single-conductor constant-parameter (CP) line with a characteristic impedance of 200 Ω [21]. The tower footing impedance is modeled as a 25-Ω lumped resistance. The insulator strings are simulated using the EMTP-RV flashover switch gap model.

D. Insulation flashover

The insulation flashover is simulated making using of the EMTP-RV air gap leader model. Its breakdown voltage-time characteristic is governed by the leader model of Shindo-Suzuki (e.g., [22]) and its performance is validated with the CIGRE equation (e.g., [23]) in the simulation environment.

E. Lightning return stroke current

The current associated with a first return stroke is considered and modeled by an ideal current source in parallel with a 1-kΩ resistance [24]. This paper employs the CIGRE recommended current waveform (e.g., [20]), which is expressed by two functions respectively describing

i) the current front:

$$I(t) = At + Bt^n, \tag{12}$$

ii) the current tail:

$$I(t) = I_1 e^{-(t-t_n)/t_1} + I_2 e^{-(t-t_n)/t_2}. \tag{13}$$

The constants in (12) and (13) are functions of the return stroke current parameters including *i)* the peak current I_{max}, *ii)* the maximum steepness S_{max}, *iii)* the front time t_f, and *iv)* the time to half value t_h. The following simulations consider the typical average values of these parameters [20].

TABLE II: Average Values of First Return Stroke Parameters

Parameter	Value	Unit
I_{max}	31	kA
S_{max}	26	kA/μs
t_f	3	μs
t_h	75	μs

IV. Application Cases

A. Power network

As illustrated in Fig. 1, the considered line setup is a 20.5-km 220-kV single-circuit overhead transmission line, whose two terminals are connected to power transformers. The line is divided into two sections. Section 1 ranging from the initial end to 12.5 km is assumed to be the potential lightning strike zone in the following simulation cases.

Note that the line terminal positioned at $x = 0$ is selected as the observation point (OP). The guessed flashover locations (GFLs) $x_{\mathbb{G}}$ are defined including the two line terminals and the overhead-line towers (OLTs), which are spaced with 500-m spans in Section 1 and 2-km spans in Section 2.

B. Simulation cases

1) Single flashover

In the first simulation case, the performance of the MCCS metric is evaluated by considering a shielding failure scenario

wherein a lightning flash bypasses the OHGWs and strikes one of the phase conductors.

To be specific, a direct lightning strike to phase a is supposed to occur at x = 6.95 km, resulting in an insulation flashover on the same phase of the nearest tower located at x = 7 km (e.g., Tower 14). The resulting transient voltages measured at the OP are presented in Fig. 2.

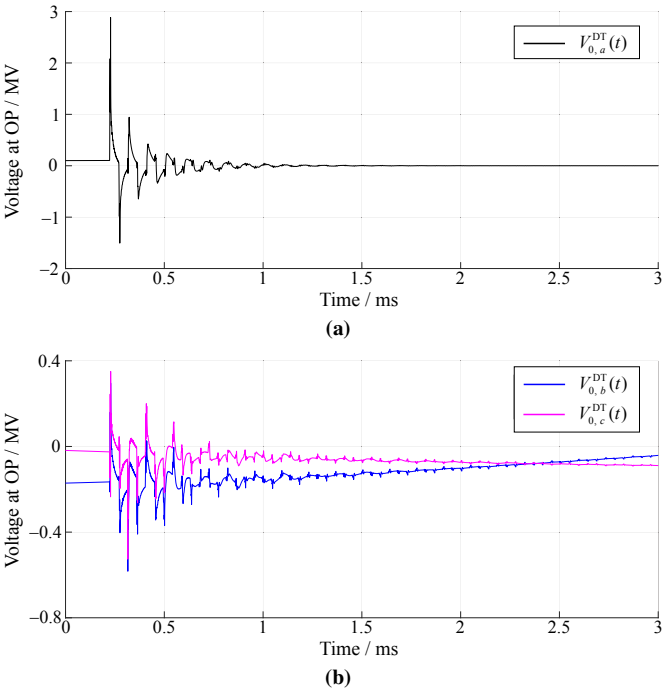

Fig. 2: Lightning strike to phase conductor resulting in a flashover on the insulator string of phase a. Transient voltages recorded at the observation point located at x = 0. (a) Phase a (flashover phase). (b) Phase b and c.

As shown in Fig. 2, the high-frequency transients [i.e., $\tilde{V}^{\mathrm{DT}}_0(t)$] are superimposed to the power-frequency (i.e., 50 Hz) components. According to Step *ii)* of the EMTR-MCCS algorithm, a 4th-order Butterworth high-pass FIR filter is applied to filter out the 50-Hz component. The extracted transients in a duration of 1 ms are time reversed and back injected into the network model to simulate the transverse branch currents at the pre-defined GFLs (see Fig. 1).

Before calculating the MCCS metric (9) to identify the most likely flashover location, the similarity characteristic is illustrated in Fig. 3 in which $I^{\mathrm{RT}}_{x_{\mathbb{G}}}(t)$ with $I^{\mathrm{TR}}_0(t)$ are plotted by considering 3 different guessed locations: Tower 4, Tower 14 (i.e., the flashover location) and Tower 21. For the sake of simplicity, only the currents of phase a are plotted.

It can be observed that, among the three GFLs including Towers 4, 14 and 21, the current at the real flashover location x_f behaves approximately as a scaled and time-delay copy of $I^{\mathrm{TR}}_{0,a}(t)$. The observation is validated by the calculated MCCS metric, which is presented as a function of GFL in Fig. 4. The flashover occurrence at phase a of Tower 14 is identified, as demonstrated by the global maximum of the MCCS metric values at this location.

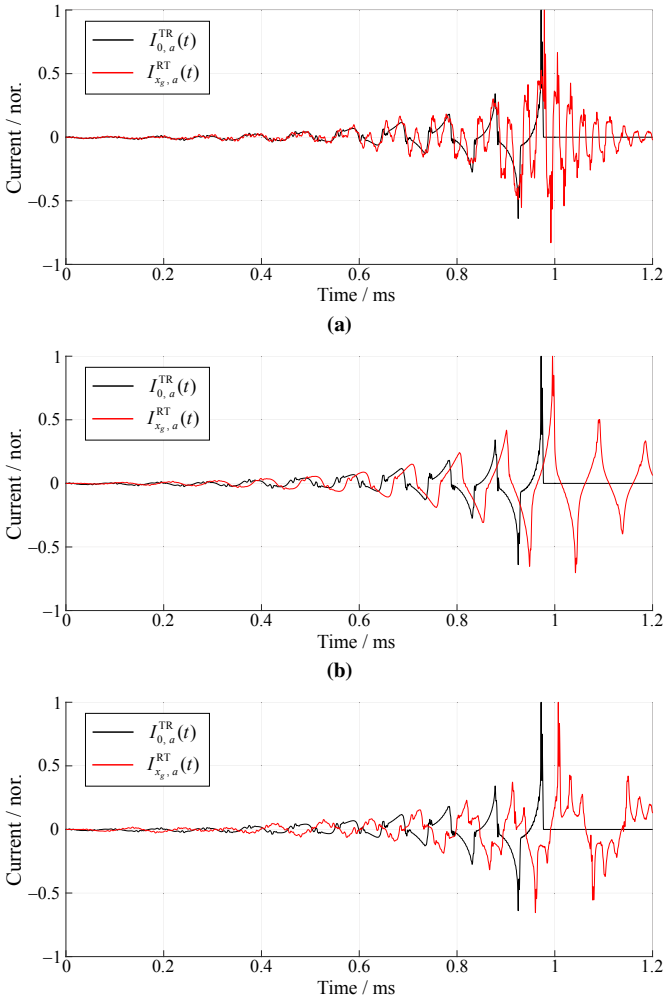

Fig. 3: Normalized waveforms of $I^{\mathrm{TR}}_{0,a}(t)$ and $I^{\mathrm{RT}}_{x_g,a}(t)$ are superimposed on same subfigures. (a) x_g = 2 km (i.e., Tower 4). (b) $x_g = x_f$ (i.e., the real flashover location at Tower 14). (c) x_g = 10.5 km (i.e., Tower 21). The normalization is based on the respective maximum amplitude.

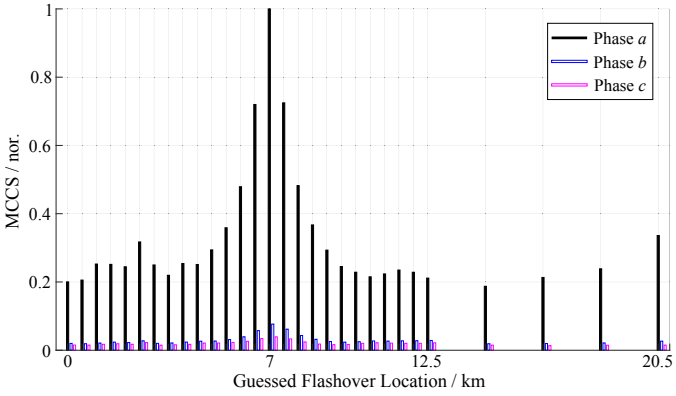

Fig. 4: Normalized MCCS metric values calculated in the case of a direct lightning strike to phase a at 6.95 km, resulting in a single flashover occurring in the nearest tower located at 7 km (Tower 14). The normalization is based on the maximum of all the three phases.

2) Single back-flashover

The second simulation involves a back-flashover (BFO). The presented case considers a direct lightning strike to Tower 13 situated at $x = 6.5$ km, resulting in a single back-flashover on the insulator string of phase b of the tower.

Fig. 5 presents the obtained MCCS metric values at the guessed flashover locations. In agreement with (10), the MCCS metric is maximized for phase b at Tower 13, which corresponds to the real location of the flashover.

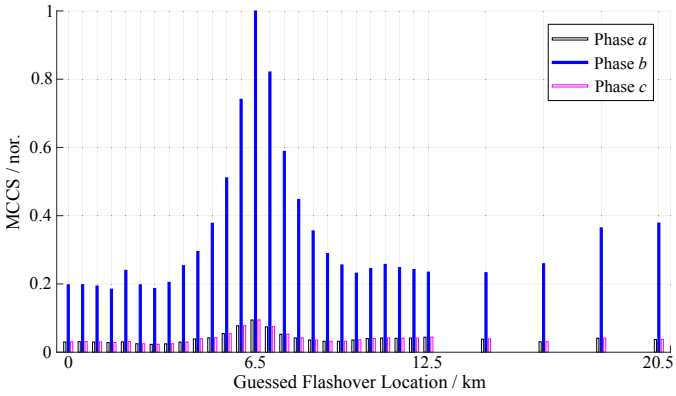

Fig. 5: Normalized MCCS metric values calculated in the case of a direct lightning strike to Tower 13 with a single back-flashover on the insulator string of phase b. The normalization is based on the maximum of all the three phases.

In summary, the MCCS metric has accurately identified the simulated flashover events by providing the correct information about the flashover location as well as the flashover phase. Moreover, a better-than-500-m (the span between two towers) location accuracy is achieved in both cases.

V. Conclusions

We presented an electromagnetic time reversal based method to locate flashovers resulting from direct lightning strikes to overhead transmission lines. The method considers the time-domain similarity between the flashover-originated high-frequency transient current and the transverse branch current observed at the flashover location. A cross-correlation metric was used to quantitatively represent the proposed similarity characteristic and to identify the location of the flashover occurrence. The performance of the similarity metric was numerically illustrated using two simulation case studies involving a shielding failure and a back-flashover, respectively. Further studies are needed to evaluate the influence of nonlinear characteristics of power network components (like surge arrester) on the performance of the EMTR-MCCS method, as well as the presence of multiple flashovers along the line.

VI. Acknowledgment

This work has been supported by the Swiss Competence Center for Energy Research FURIES (Future Swiss Electrical Infrastructure).

References

[1] "IEEE Guide for Improving the Lightning Performance of Transmission Lines," *IEEE Std 1243-1997*, pp. 1–44, Dec 1997.

[2] V. Cooray, ed., *The Lightning Flash*. IET, 2 ed., 2008.

[3] L. van der Sluis, *Transients in Power Systems*. John Wiley & Sons, 2001.

[4] F. Napolitano, A. Borghetti, M. Paolone, and M. Bernardi, "Voltage transient measurements in a distribution network correlated with data from lightning location system and from sequence of events recorders," *Electric Power Systems Research*, vol. 81, no. 2, pp. 237 – 253, 2011.

[5] A. Borghetti, C. A. Nucci, M. Paolone, and M. Bernardi, "A statistical approach for estimating the correlation between lightning and faults in power distribution systems," in *2006 International Conference on Probabilistic Methods Applied to Power Systems*, pp. 1–7, June 2006.

[6] P. Barker and C. W. Burns, "Photographs helps solve the distribution lightning problems," *IEEE Power Engineering Review*, vol. 13, pp. 23–26, June 1993.

[7] D. Chanda, N. K. Kishore, and A. K. Sinha, "A wavelet multiresolution-based analysis for location of the point of strike of a lightning overvoltage on a transmission line," *IEEE Transactions on Power Delivery*, vol. 19, pp. 1727–1733, Oct 2004.

[8] R. E. Jimnez and J. G. Herrera, "Location of direct lightning impacts to overhead transmission lines by means of a time of arrival algorithm," in *2012 North American Power Symposium (NAPS)*, pp. 1–6, Sep. 2012.

[9] R. Razzaghi, M. Scatena, K. Sheshyekani, M. Paolone, F. Rachidi, and G. Antonini, "Locating lightning strikes and flashovers along overhead power transmission lines using electromagnetic time reversal," *Electric Power Systems Research*, vol. 160, pp. 282 – 291, 2018.

[10] G. Lugrin, N. M. Mora, F. Rachidi, M. Rubinstein, and G. Diendorfer, "On the location of lightning discharges using time reversal of electromagnetic fields," *IEEE Transactions on Electromagnetic Compatibility*, vol. 56, pp. 149–158, Feb 2014.

[11] N. Mora, F. Rachidi, and M. Rubinstein, "Application of the time reversal of electromagnetic fields to locate lightning discharges," *Atmospheric Research*, vol. 117, pp. 78 – 85, 2012. Special Issue dedicated to the 30th International Conference on Lightning Protection (ICLP).

[12] R. Razzaghi, G. Lugrin, H. Manesh, C. Romero, M. Paolone, and F. Rachidi, "An efficient method based on the electromagnetic time reversal to locate faults in power networks," *IEEE Transactions on Power Delivery*, vol. 28, pp. 1663–1673, July 2013.

[13] A. Codino, Z. Wang, R. Razzaghi, M. Paolone, and F. Rachidi, "An alternative method for locating faults in transmission line networks based on time reversal," *IEEE Transactions on Electromagnetic Compatibility*, vol. 59, pp. 1601–1612, Oct 2017.

[14] Z. Wang, S. He, Q. Li, B. Liu, R. Razzaghi, M. Paolone, Y. Xie, M. Rubinstein, and F. Rachidi, "A full-scale experimental validation of electromagnetic time reversal applied to locate disturbances in overhead power distribution lines," *IEEE Transactions on Electromagnetic Compatibility*, vol. 60, pp. 1562–1570, Oct 2018.

[15] Z. Wang, A. Codino, R. Razzaghi, M. Paolone, and F. Rachidi, "Using electromagnetic time reversal to locate faults in transmission lines: Definition and application of the mirrored minimum energy property," in *2017 International Symposium on Electromagnetic Compatibility - EMC EUROPE*, pp. 1–6, Sep. 2017.

[16] M. Fink, "Time reversal of ultrasonic fields. i. basic principles," *IEEE Transactions on Ultrasonics, Ferroelectrics, and Frequency Control*, vol. 39, pp. 555–566, Sep. 1992.

[17] J. de Rosny, G. Lerosey, and M. Fink, "Theory of electromagnetic time-reversal mirrors," *IEEE Transactions on Antennas and Propagation*, vol. 58, pp. 3139–3149, Oct 2010.

[18] M. P. Farhad Rachidi, Marcos Rubinstein, ed., *Electromagnetic Time Reversal: Application to EMC and Power Systems*. John Wiley & Sons, 2017.

[19] Z. Wang, R. Razzaghi, M. Paolone, and F. Rachidi, "Electromagnetic time reversal applied to fault location: On the properties of back-injected signals," in *2018 Power Systems Computation Conference (PSCC)*, pp. 1–7, June 2018.

[20] "Guide to Procedures for Estimating the Lightning Performance of Transmission lines," *Report of WG 1*, CIGRE, 1991.

[21] J. A. Martinez-Velasco, ed., *Transient Analysis of Power Systems: Solution Techniques, Tools and Applications*. Wiley-IEEE, 2015.

[22] T. Shindo and T. Suzuki, "A new calculation method of breakdown voltage-time characteristics of long air gaps," *IEEE Transactions on Power Apparatus and Systems*, vol. PAS-104, pp. 1556–1563, June 1985.
[23] "Lightning protection of UHV transmission lines," *Report of WG 33.01*, CIGRE, 1997.
[24] V. A. Rakov, "Some inferences on the propagation mechanisms of dart leaders and return strokes," 1998.